

Supporting Information

Construction and Application of α -Fe₂O₃ Nanocubes Dominated by the Composite Interaction between Polyvinyl Chloride and Potassium Ferrocyanide

Pu Du^a, Le Xin Song^{*a,b}, Juan Xia^{*b}, Yue Teng^b and Zheng Kun Yang^a

^aDepartment of Chemistry, University of Science and Technology of China, Jin Zhai Road 96, Hefei 230026, China

^bCAS Key Laboratory of Materials for Energy Conversion, Department of Materials Science and Engineering, University of Science and Technology of China, Jin Zhai Road 96, Hefei 230026, China

solexin@ustc.edu.cn xiajuan@mail.ustc.edu.cn

A list of the contents for all the Supporting Information

Pages	Contents
1	A table of contents page.
2	Fig. S1 XRD pattern of the α -Fe ₂ O ₃ nanoparticles obtained by sintering PF at 800 K for 8 h.
3	Fig. S2 FE-SEM image of the α -Fe ₂ O ₃ nanoparticles obtained by sintering PF at 800 K for 8 h.
4	Fig. S3 XRD patterns of the α -Fe ₂ O ₃ nanoparticles obtained by sintering PVC/PF-10 (a) and PVC/PF-50 (b) at 800 K for 8 h.
5	Fig. S4 FE-SEM images of the α -Fe ₂ O ₃ nanoparticles obtained by sintering PVC/PF-10 (a) and PVC/PF-50 (b) at 800 K for 8 h.
6	Fig. S5 XRD pattern of the α -Fe ₂ O ₃ nanoparticles and carbon obtained by sintering PVC/PF-20 in a sealed muffle furnace environment at 500 K for 1 h.
7	Fig. S6 Raman spectra of the α -Fe ₂ O ₃ nanomaterials obtained at 500, 550, 600, 700 and 800 K for 1 h.
8	Fig. S7 The XRD pattern and SEM image of the α -Fe ₂ O ₃ obtained by sintering the PVC/PF-20 at 900 K for 1 h.
9	Fig. S8 FE-SEM image of the α -Fe ₂ O ₃ nanoparticles obtained by sintering free PF at 600 K for 1 h.
10	Fig. S9 DSC (A) and DMA (B) curves of the PVC/PF-20 at the temperature from 335~380 K.
11	Fig. S10 TG curves of free PVC and the PVC/PF-20 under nitrogen atmosphere.
12	Fig. S11 The TG curve of the PVC/PF-20 under air.
13	Fig. S12 N ₂ adsorption-desorption isotherms of the α -Fe ₂ O ₃ nanocubes (A) and nanoparticles (B).

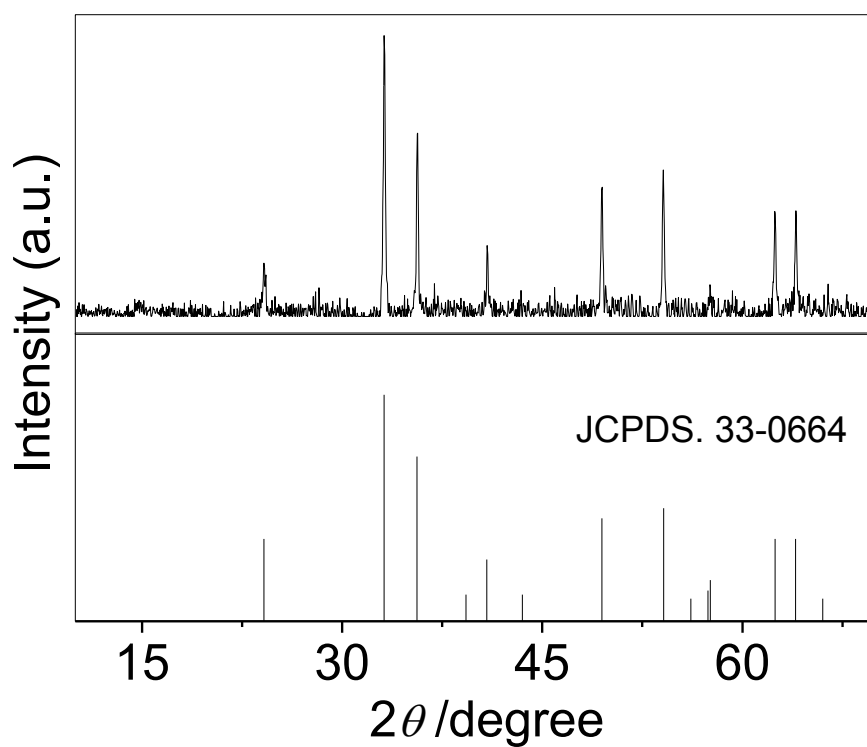


Fig. S1 XRD pattern of the α -Fe₂O₃ nanoparticles obtained by sintering PF at 800 K for 8 h.

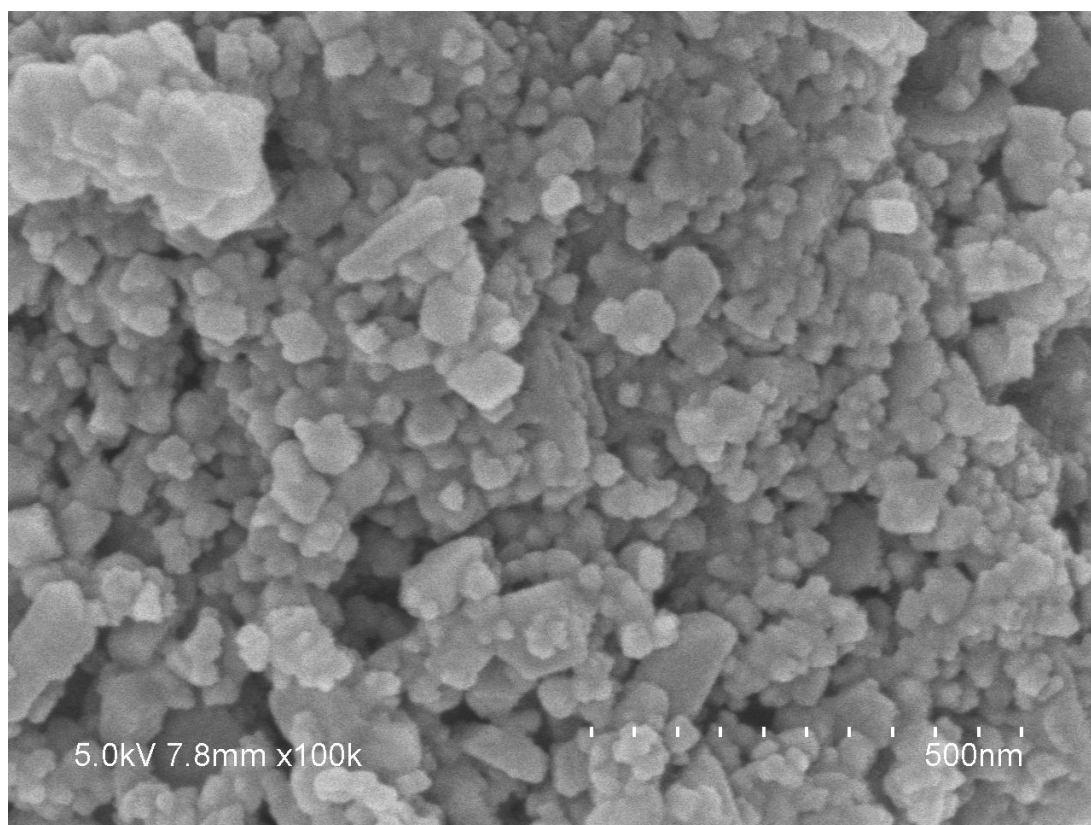


Fig. S2 FE-SEM image of the α -Fe₂O₃ nanoparticles obtained by sintering PF at 800 K for 8 h.

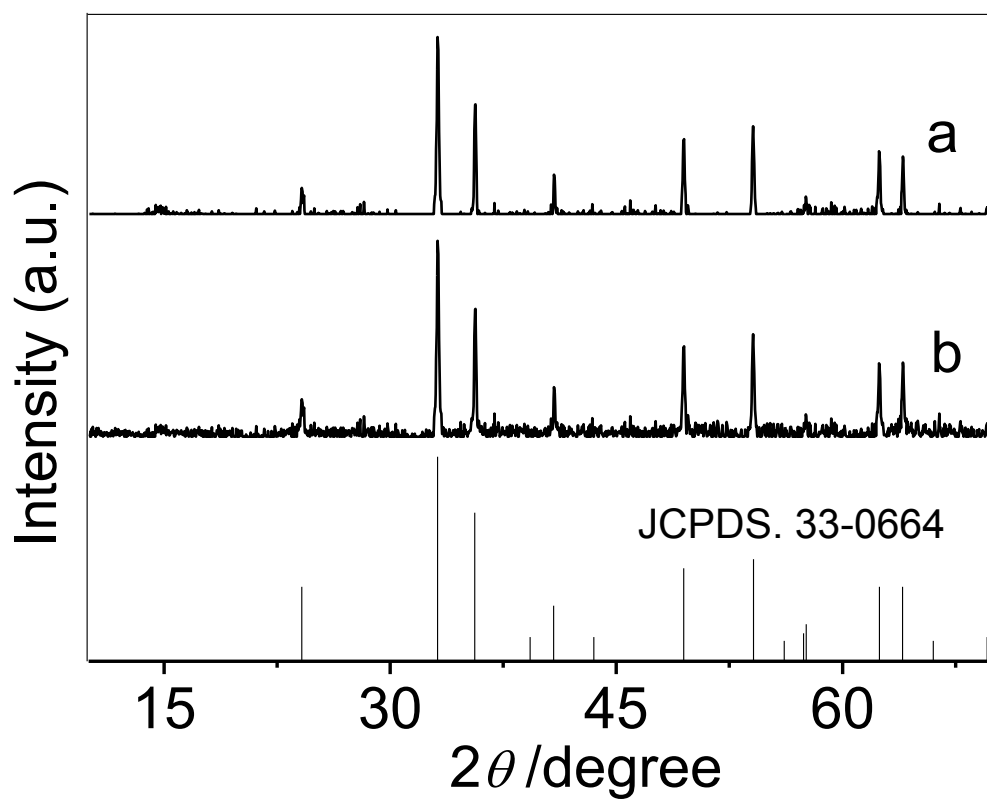


Fig. S3 XRD patterns of the α -Fe₂O₃ nanoparticles obtained by sintering PVC/PF-10 (a) and PVC/PF-50 (b) at 800 K for 8 h.

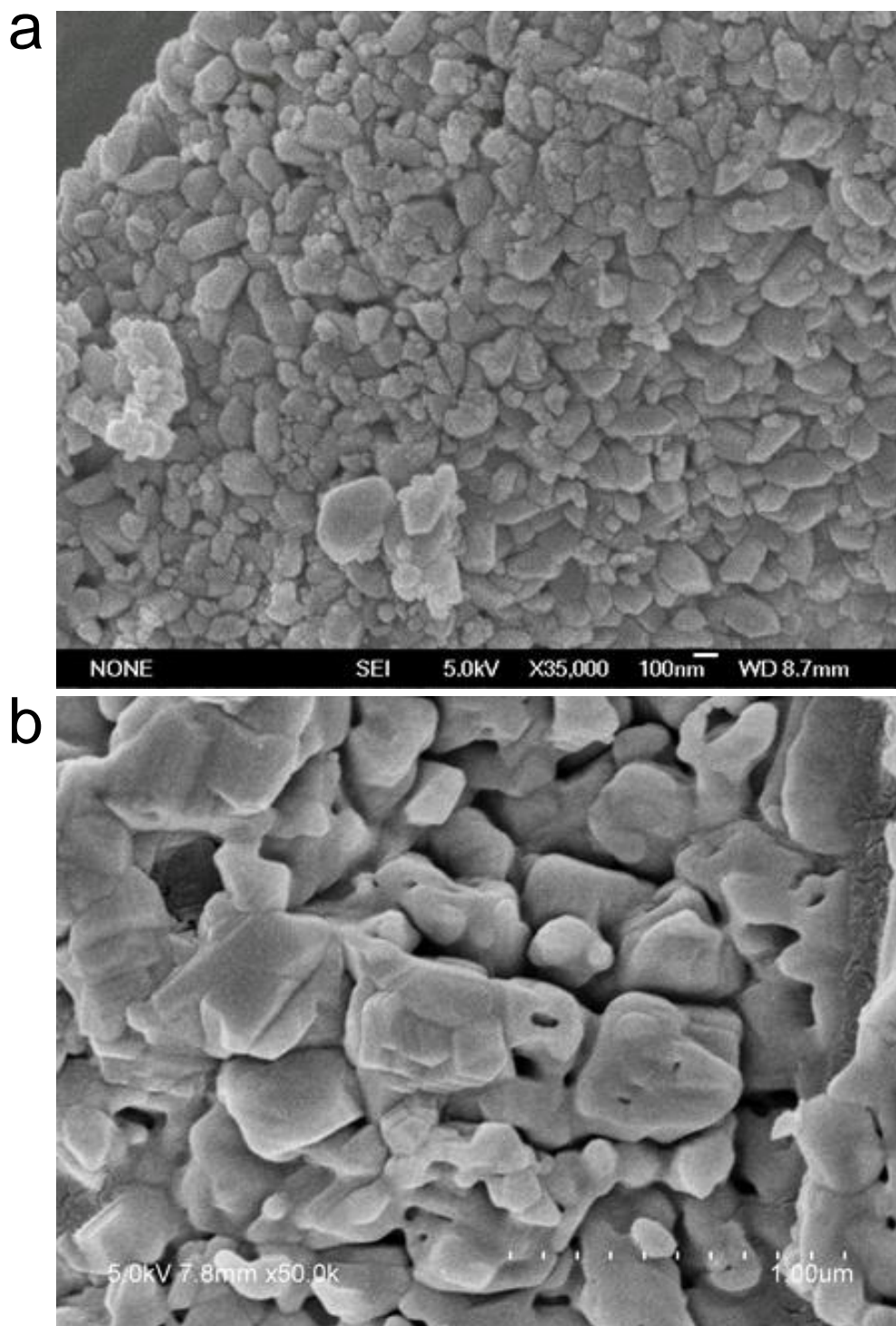


Fig. S4 FE-SEM images of the α -Fe₂O₃ nanoparticles obtained by sintering PVC/PF-10 (a) and PVC/PF-50 (b) at 800 K for 8 h.

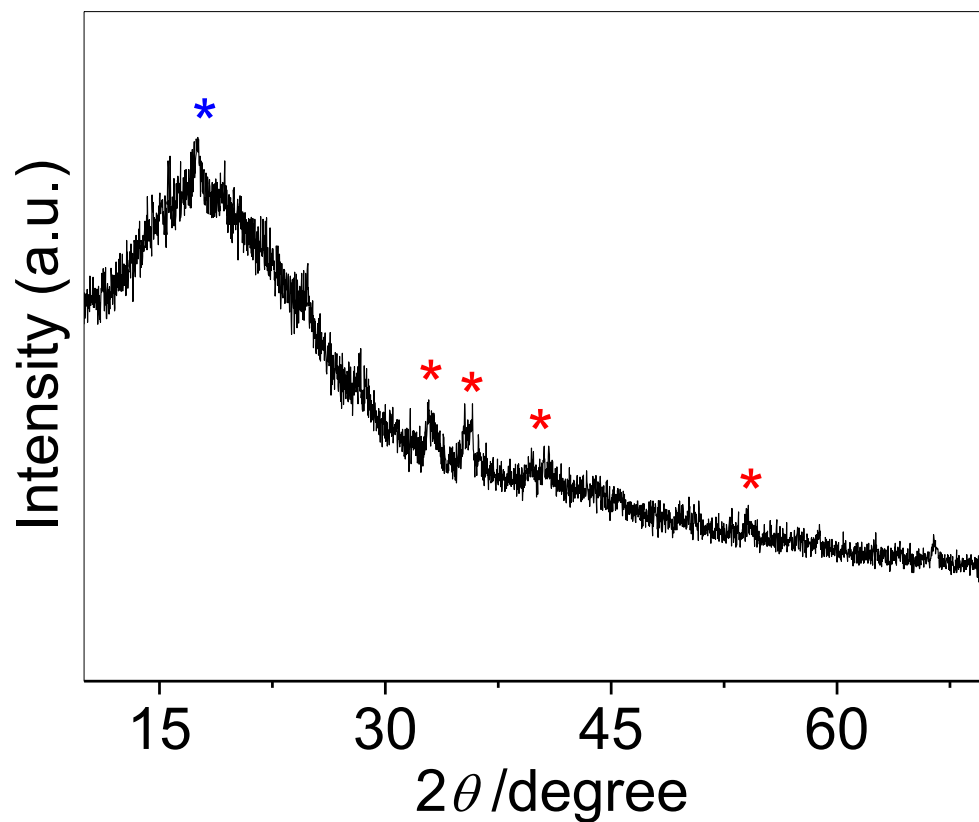


Fig. S5 XRD pattern of the α -Fe₂O₃ nanoparticles and carbon obtained by sintering PVC/PF-20 in a sealed muffle furnace environment at 500 K for 1 h (the blue asterisk denotes the peak of carbon and the red asterisks denote the peaks of α -Fe₂O₃ nanoparticles).

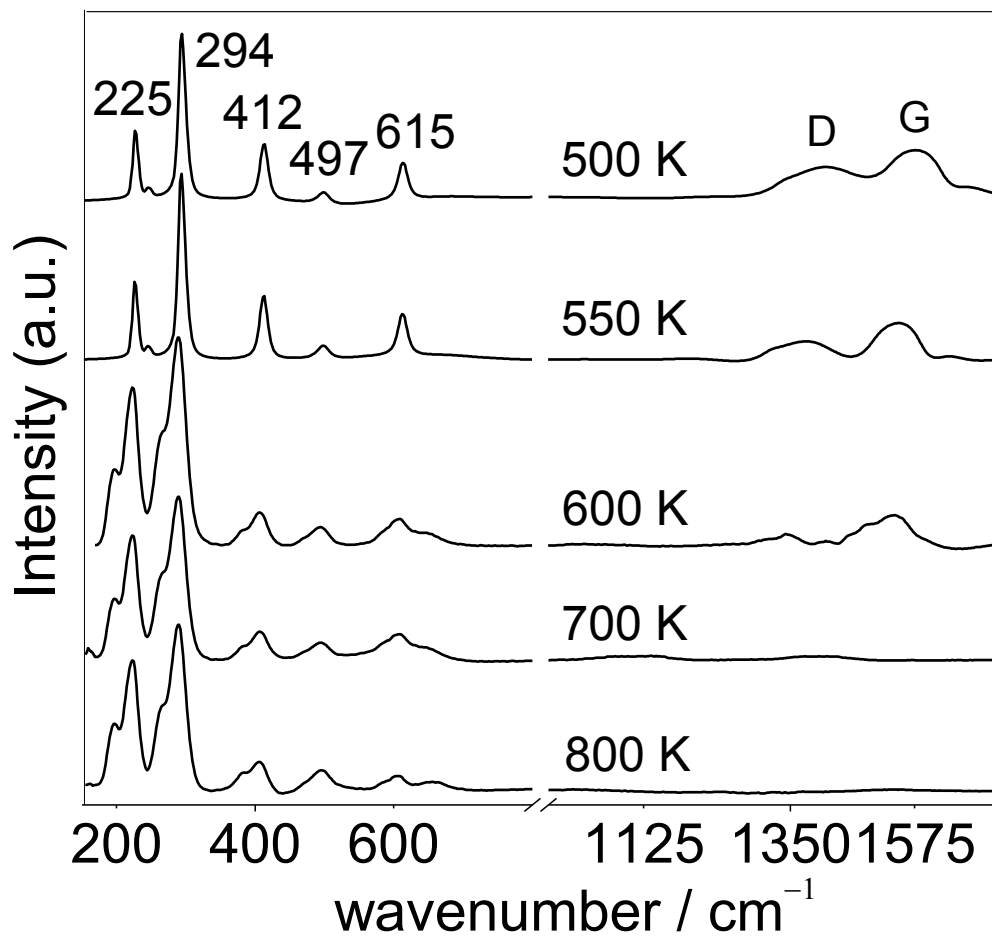


Fig. S6 Raman spectra of the α -Fe₂O₃ nanomaterials obtained at 500, 550, 600, 700 and 800 K for 1 h.

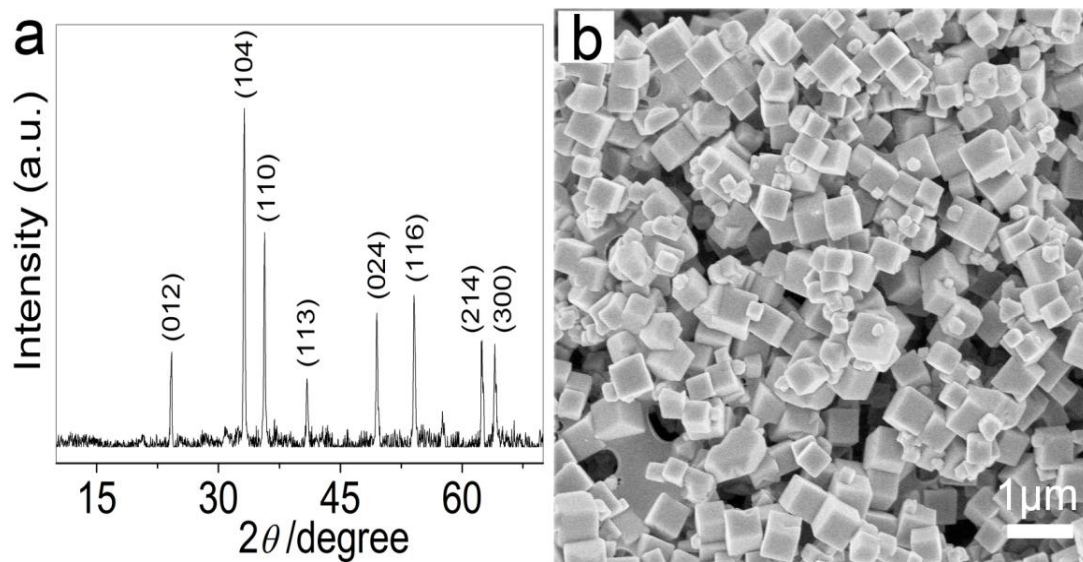


Fig. S7 The XRD pattern and SEM image of the $\alpha\text{-Fe}_2\text{O}_3$ obtained by sintering the PVC/PF-20 at 900 K for 1 h.

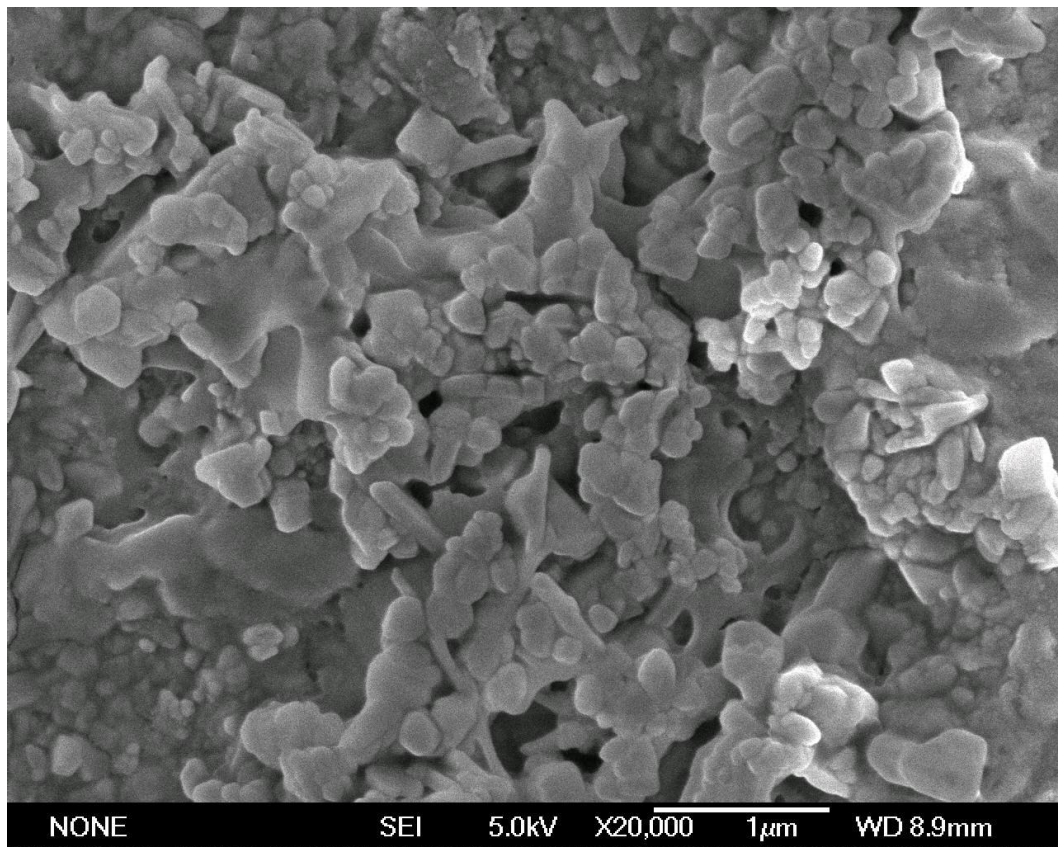


Fig. S8 FE-SEM image of the α -Fe₂O₃ nanoparticles obtained by sintering free PF at 600 K for 1 h.

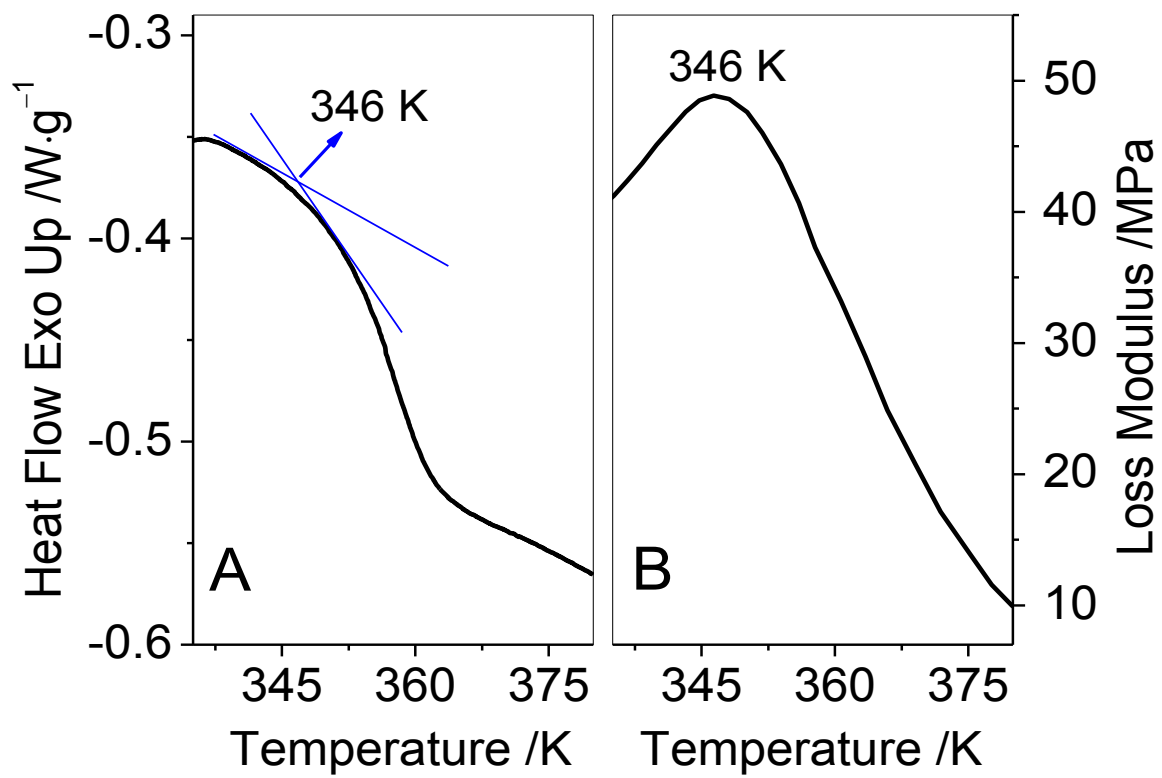


Fig. S9 DSC (A) and DMA (B) curves of the PVC/PF-20 at the temperature from 335~380 K.

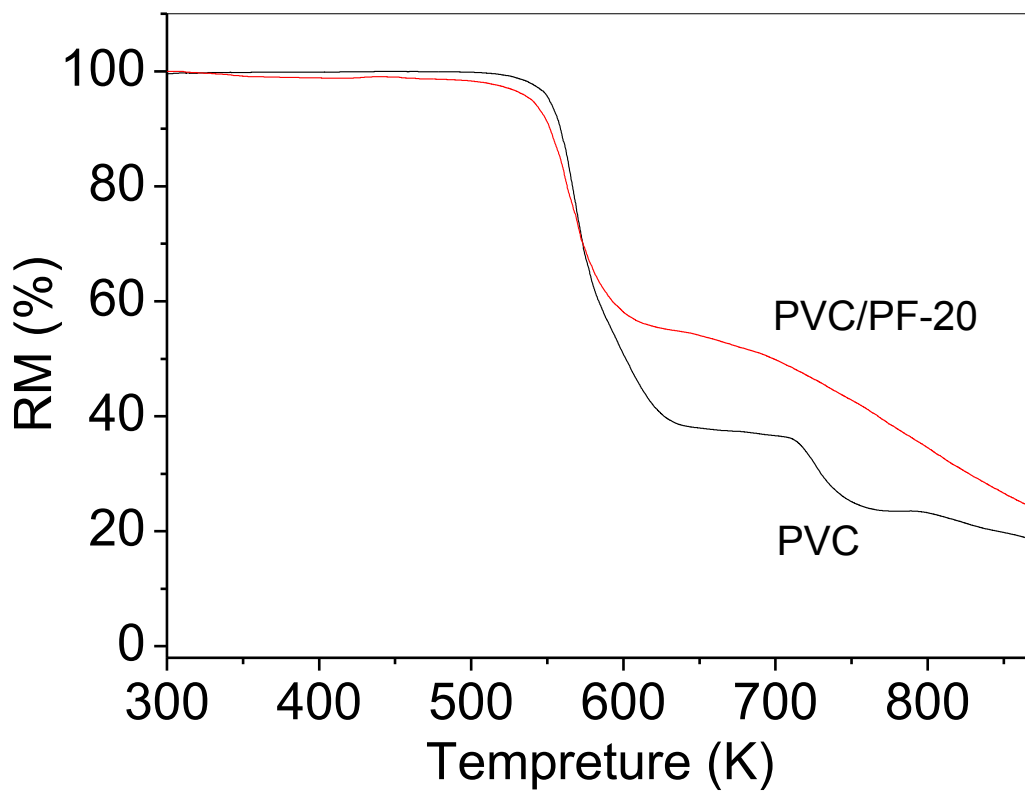


Fig. S10 TG curves of free PVC and the PVC/PF-20 under nitrogen atmosphere.

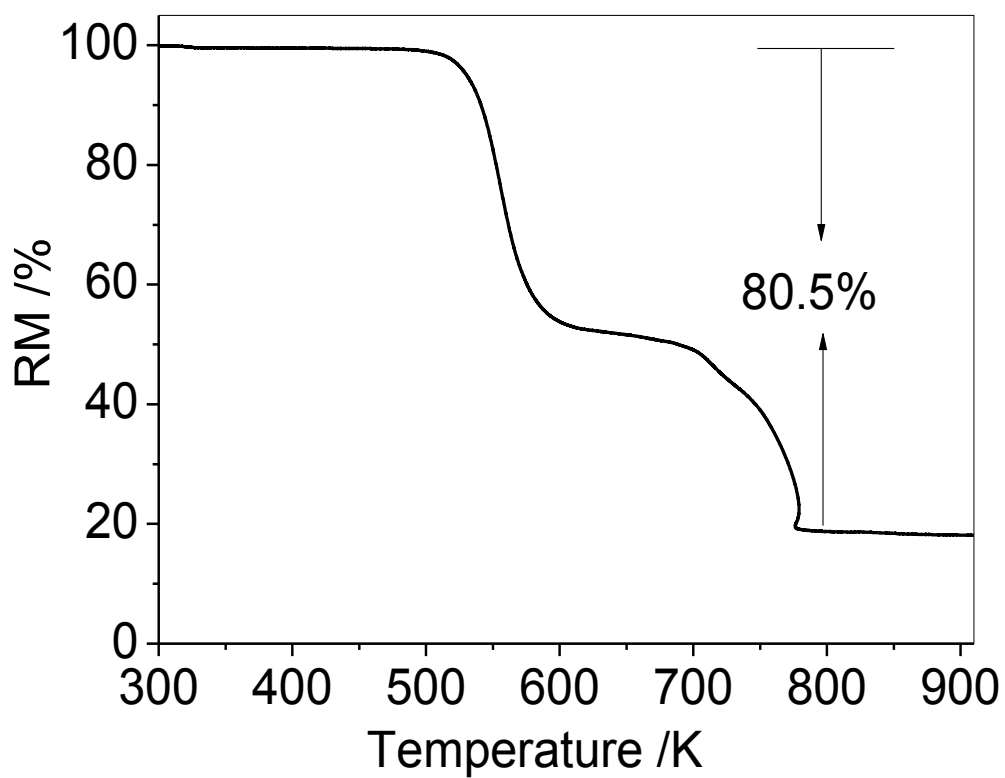


Fig. S11 The TG curve of the PVC/PF-20 under air.

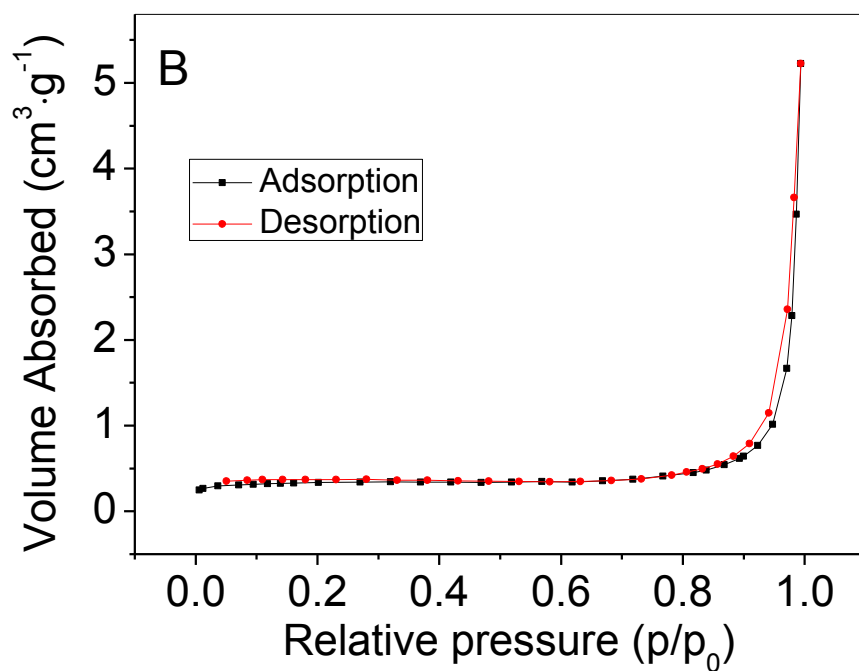
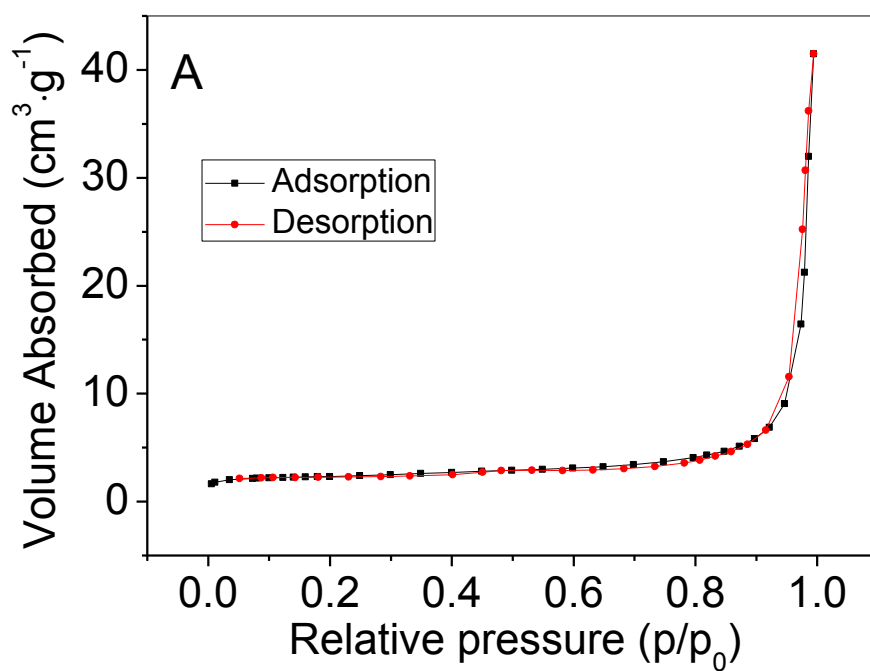


Fig. S12 N_2 adsorption-desorption isotherm of the $\alpha\text{-Fe}_2\text{O}_3$ nanocubes (A) and nanoparticles (B).